Respiratory Research

RESEARCH

Open Access

Mechanistic insights into the role of EGLN3 in pulmonary vascular remodeling and endothelial dysfunction

Xiaodong Deng[1], Qing Que[1], Kunchi Zhang[1], Bo Li[1], Nianlong Yang[1], Qiang Hu[1], Sheng Lv[1] and Yi Liu[1*]

Abstract

Endothelial dysfunction is a pivotal initiating factor in vascular remodeling in pulmonary hypertension. EGLN3, a hypoxia response factor, plays a significant role in cell proliferation and angiogenesis, which are closely related to the pathophysiological conditions of pulmonary hypertension. This study investigates the potential involvement of EGLN3 in the injury response of pulmonary vascular endothelial cells and its contribution to the development of pulmonary arterial hypertension. Research has demonstrated that in patients with pulmonary arterial hypertension and various animal models of the condition, EGLN3 expression is upregulated in the remodeled pulmonary artery endothelium. Notably, the endothelial cell-specific knockout of EGLN3 can decelerate the progression of pulmonary arterial hypertension, whereas its overexpression has the opposite effect. Mechanistic analyses reveal that under hypoxic conditions, JUN initiates the transcription of EGLN3 by binding to its promoter region. Subsequently, EGLN3 interacts with HUR to enhance the stability of EGFR mRNA, thereby activating the PI3K/AKT and MAPK signaling pathways, which ultimately results in endothelial cell damage, proliferation, and migration. These findings suggest that EGLN3 is a critical gene for maintaining endothelial function and vascular homeostasis and holds promise as a novel therapeutic target for the treatment of pulmonary hypertension.

Highlights

- The study elucidated the role of EGLN3 in PH.
- This study explored the relationship between EGLN3 and HUR.
- This study revealed that EGLN3 transcription was promoted by JUN under hypoxic conditions.

Keywords PH, EGLN3, EGFR, HUR, mRNA stability

*Correspondence:
Yi Liu
yi603915991@163.com

Graphical Abstract

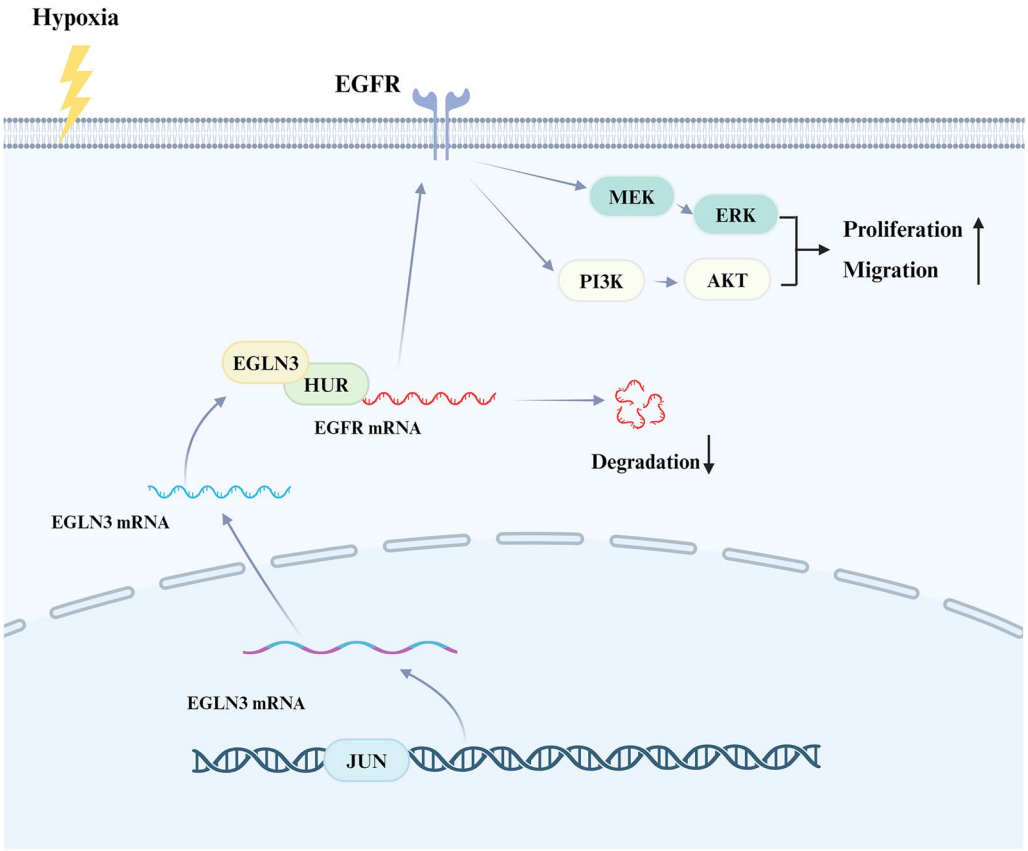

Introduction

Pulmonary hypertension (PH) is a progressive cardiopulmonary disease characterized by the remodeling of pulmonary vessels, muscularization of distal small vessels, and changes in the right ventricle [1, 2]. The pathogenesis of PH involves various cell types, including pulmonary artery endothelial cells (PAECs), vascular smooth muscle cells, and macrophages, as well as multiple contributing factors such as genetic predisposition, DNA damage, hypoxia, and inflammation [3, 4]. Among these cell types, PAECs are considered primary initiators of vascular remodeling. Injury to PAECs can activate numerous molecular signaling pathways. Consequently, these cells respond to various injury environments and transmit a range of signaling molecules, including cytokines and exosomes, that regulate pathological changes in other cells [5, 6]. Consequently, improving endothelial dysfunction is a central focus in exploring the mechanisms underlying PH. In this context, we hypothesize that an unidentified pathogenic protein, highly expressed in the PAECs of patients with PH, may promote remodeling of both the pulmonary artery and the right ventricle.

We analyzed the GEO163827 dataset to identify new pathogenic proteins and discovered that Egl-9 family hypoxia-inducible factor 3 (EGLN3) protein expression was significantly upregulated in human PAECss (hPAECs) following hypoxic injury. Additionally, EGLN3 expression was elevated in the lungs of patients with PH, in mice with hypoxia-induced PH, and in rats with Monocrotaline (MCT)-induced PH. EGLN3, a member of the EGL-9 prolyl hydroxylase family, is notably induced under hypoxic conditions [7]. This protein regulates various cellular processes, including cell signaling, cell cycle, apoptosis, proliferation, and migration, and plays a crucial role in tumor growth, progression, and angiogenesis [8, 9]. Although EGLN3 can be induced under various physiological and pathological conditions, its biological function remains largely unexplored. Whether EGLN3 contributes to the development of PH remains uncertain.

The epidermal growth factor has emerged in recent years as a significant factor in the pathogenesis of

pulmonary arterial hypertension. The growth factors and other receptor tyrosine kinases are being investigated as therapeutic targets for cardiopulmonary diseases [10–12]. Studies have shown that various epidermal growth factor receptor (EGFR) inhibitors, such as gefitinib and erlotinib, can significantly reduce vascular and right ventricular remodeling in rats with MCT- and hypoxia-induced PH, thereby effectively lowering pulmonary artery pressure [13, 14]. Our research indicates that EGLN3 is significantly positively correlated with EGFR expression in PAECs, and the stability of EGFR mRNA is enhanced in EGLN3-overexpressing cell lines. This finding suggests a role of EGLN3 in mediating EGFR mRNA stability; however, the specific mechanism of this regulation remains unclear.

In this study, we analyzed public transcriptome sequencing data related to PH and found significant upregulation of EGLN3 in hypoxia-induced endothelial cells. Experimental data indicated a positive correlation of high EGLN3 expression levels with the severity of PH. Further mechanistic studies revealed that EGLN3 enhanced the stability of its mRNA by binding to ELAV-like RNA-binding protein 1 (HUR). This interaction activated the downstream PI3K/Akt and MEK/ERK signaling pathways, thereby promoting the proliferation and migration of endothelial cells. Using the JASPAR (https://jaspar.genereg.net/) and PROMO (https://alggen.lsi.upc.es/cgi-bin/promo_v3/promo/promoinit.cgi?dirDB=TF_8.3) databases, we identified the key transcription factor Jun proto-oncogene (JUN) as a regulator of EGLN3 under hypoxic conditions. Consequently, this study established a novel molecular regulatory axis in pulmonary arterial hypertension and suggested that targeting EGLN3 at the gene level could significantly ameliorate the condition and present a new avenue for drug development.

Materials and methodsmethods

Animals

The Tie2-Cre mouse strain was sourced from Genechem Co., Ltd.,. The strain was employed to generate endothelial cell-specific EGLN3 knockout mice ($EGLN3^{EC-KO}$). $EGLN3^{EC-KO}$ mice were produced by crossing Tie2-Cre with $EGLN3^{floxed/floxed}$ mice. Following this initial cross, the resulting Tie2-$CreEGLN3^{floxed/+}$ mice were backcrossed with $EGLN3^{floxed/floxed}$ mice. This breeding strategy ultimately produced Tie2-$CreEGLN3^{floxed/floxed}$ mice, which were designated as $EGLN3^{EC-KO}$ mice. $EGLN3^{floxed/floxed}$ mice were used as control mice, designated as $EGLN3^{WT}$ mice.

Additionally, AAV9-EGLN3-loxp (AAV9-EGLN3) and its corresponding negative control, AAV9 NC-loxp (AAV9-NC), were both developed by Genechem Co., Ltd. The Tie2-Cre rats were administered AAV9-EGLN3 (1E + 11 viral genomes per rat) and AAV9-NC (1E + 11 viral genomes per rat) through a single injection into the tail vein to create endothelial cell–specific EGLN3 overexpression in rats. Following this treatment, the rats were monitored for more than 28 days. The control groups received only the vehicle, allowing for a clear comparison between the experimental and control conditions.

PH models in rodents

A mouse model of hypoxic pulmonary hypertension was constructed by placing EGLN3EC-KO mice and age-matched EGLN3WT mice in a ventilation chamber (Oxycycler Model A84XOV; BioSpherix, Ltd., China). The ventilation chamber was capable of regulating oxygen concentration to either normal (21%) or hypoxic (10%) levels. The chamber was opened twice weekly for 10 min each time to clean the ventilation area and replenish food and water.

After 4 weeks of culture, the Sprague–Dawley (SD) rats injected with AAV9 adeno-associated virus reached a weight of 200–250 g and demonstrated stable expression of EGLN3. Subsequently, each rat was intraperitoneally injected with monocrotaline (MCT) at a dose of 60 mg/kg. Pulmonary hypertension gradually developed from day 0 to day 14. As a vehicle control, rats in the control group received intraperitoneal injections of normal saline. Following 14 days of MCT induction, the rats were sacrificed for measuring indicators such as right ventricular pressure, as described in the subsequent section.

Parameter measurement

The rats were sacrificed by injecting 40 mg/kg of sodium pentobarbital intraperitoneally. Next, a pre-filled heparin copper PE-50 catheter (Taimeng, Chengdu, China) was carefully inserted into the right external jugular vein. Right ventricular systolic pressure (RVSP, mm Hg) was measured by connecting the distal end of the catheter to a multiconductor physiological recorder (Taimeng, Chengdu, China) through a pressure transducer. The recording of RVSP served serve as an indirect indicator of pulmonary arterial systolic pressure. The right ventricle (RV) was separated from the left ventricle (LV) and the septum (S). The RV/(LV + S) ratio, indicative of the extent of RV hypertrophy (RVHI), was determined by weighing these specimens. The right lung was collected, immediately snap-frozen using liquid nitrogen, and then stored at − 80 °C for subsequent biochemical analyses. The left lung underwent initial perfusion with physiological saline, followed by 4% paraformaldehyde. It was then excised and submerged in 4% paraformaldehyde for 72 h. Subsequently, the lung was dehydrated using a gradient of 20% and 30% sucrose solutions, and finally embedded in an optimal cutting temperature (OCT) compound.

Tissue slices were stained with eosin and hematoxylin (HE), and the percentages of medial wall area (WA%) and medial wall thickness (WT%) were calculated using the following equations: WT% = (WT/external diameter) × 100; and WA% = (medial WA/ total vascular area) × 100. Each experiment was replicated at least three times.

Immunofluorescence and in vivo proliferation

Lung tissue Sects. (5 μm) were rewarmed at room temperature for 10 min and then rinsed three times with PBS to remove OCT. The sections were then treated with 0.5% Triton X-100 for 15 min, followed by three additional rinses with PBS. The goat serum was subsequently added for blocking to eliminate nonspecific binding sites. Double immunofluorescence staining was performed using primary antibodies against EGLN3(1:200 ab184714, Abcam) and VWF (an endothelial cell marker, 1:200 ab6994, Abcam). The slides were incubated with the corresponding Alexa 488 or Alexa 555-conjugated secondary antibodies, and each section was stained with 4′,6-diamidino-2-phenylindole (DAPI) for nuclear counterstaining. All images were acquired using a DM1000 fluorescence microscope (Leica, Wetzlar, Germany). Additionally, proliferating cell nuclear antigen (PCNA) was stained in the lung tissue sections to assess the proliferative capacity of human pulmonary arterial endothelial cells (hPAECs).

Human lung samples

During lung surgery for PAH complicated by cancer, lung tissues from patients were collected from an area far from the tumor margins. Informed written consent was obtained from every patient for using their lung tissues in this study.

Quantitative polymerase chain reaction

Total RNA was extracted from the pulmonary artery endothelium of mice, rats, or humans using Trizol reagent (Invitrogen) according to the manufacturer's instructions. Subsequently, total RNA was reverse transcribed (RT) into complementary DNA (cDNA) using an RT kit (beyotime), following the manufacturer's protocol. Real-time quantitative polymerase chain reaction (qPCR) analysis was conducted with SYBR Green PCR mix (beyotime, shanghai, China) and an Applied Biosystems StepOnePlus real-time PCR device (ABI 7500). Each experiment was performed a minimum of four times. Computed tomography (CT) values were obtained using the Applied Biosystems 7500 sequence detection system software, and comparative CT analysis was employed to evaluate the results. The samples were normalized to β-actin to account for the changes in cDNA loading. The PCR primer sequences are shown in Table S1.

Cell culture and transfection

hPAECs (ScienCell, Catalog, #3110) were obtained from ScienCell and cultured in an endothelial cell culture medium (ScienCell, Cat. #1001). The experiments used hPAECs in passages 3–8. Standard incubator conditions for cell culture included a temperature of 37 °C, 21% O2, 5% CO_2, and hypoxia (1% O2) for 24 h. The viruses used in this study were supplied by Genechem Co., Ltd. (China), and the knockdown sequences are detailed in Table S1. A total of 5×10^5 cells/mL were inoculated into a T25 culture flask. Following cell adhesion, lentivirus and transfection solutions were introduced. The medium was replaced after 12 h. Puromycin was added to the cells after 3 days for selection. The expression of fluorescent proteins was evaluated using fluorescence microscopy (DM1000; Leica, Wetzlar, Germany), whereas the efficacy of overexpression and knockdown was determined using Western blot analysis.

Dural luciferase reporter assay

hPAECs were transfected according to the manufacturer's protocol. Both the pcDNA3.1 EGLN3 and the empty control plasmid were introduced into the hPAECs, accompanied by pGL3-Basic vectors containing different promoters. Subsequently, the activities of Firefly and Renilla luciferase were evaluated using the Dual- Luciferase Assay Kit (Promega) 24 h after the transfection took place.

ChIP-qPCR

A Chromatin Immunoprecipitation (ChIP) Assay Kit, (Millipore) was employed to analyze specific protein-DNA interactions. The cells were fixed with 1% formaldehyde for 10 min at room temperature to facilitate the cross-linking of proteins and DNA. Subsequently, cell-derived DNA–protein complexes were sheared into fragments of 200–500 base pairs using a sonicator. The pre-cleared fragments were then exposed to 10 μg of JUN antibody or IgG as a negative control overnight, followed by precipitation with protein A. After reversing cross-links by heating at 65 °C overnight, proteinase K digestion was conducted at 45 °C for 2 h. The DNA extracted using the QIAquick PCR (beyotime) purification kit was then used to assess the affinity to the EGLN3 promoter region through qPCR, employing specific primers designed for the EGLN3 promoter region.

Co-immunoprecipitation

The cells were exposed to hypoxia for 24 h and then lysed using the co-immunoprecipitation (Co-IP) lysis buffer (Thermo Scientific). The supernatant obtained from the centrifugation of the lysate was used for Co-IP. Equal volumes of protein were incubated overnight

with anti-EGLN3, IgG (Santa Cruz), or HUR (ab200342, Abcam), followed by a 3-h incubation with Protein G Agarose Beads (Beyotime). After incubation, the beads were washed repeatedly with PBS containing 0.1% Tween 20. Finally, the SDS sample buffer was added, and the results were analyzed using Western blotting.

Western blotting

The proteins were transferred to a PVDF membrane for immunoblotting following the separation of proteins through polyacrylamide gel electrophoresis with 10% sodium dodecyl sulfate. The membrane was subsequently blocked for 1 h using a mixture of 5% skimmed milk and 0.1% Tween-20 in PBS. It was then incubated with the primary antibody for 12 h and treated with horseradish peroxidase-conjugated secondary antibodies specific to mice, rats, or rabbits for an additional hour. Chemiluminescent reagents (Pierce) were employed for all immunoblots, and signals were captured using the ChemiScope 3600MINI (Clinx Science Instruments). Details regarding the antibodies and their respective dilution ratios are as follows: JUN (1:2000 ab40766, Abcam), EGLN3 (1:2000 ab184714, Abcam), HUR (1:1000 ab200342, Abcam), EGFR (1:5000 ab52894, Abcam), PI3K(1:500, AF3242; Affinity), P-PI3K (1:1000, WL02240; Wanleibio), AKT (1:500, WL0003b; Wanleibio), P-AKT (1:500, WLP001a; Wanleibio), MRK (1:1000 WL03328, Wanleibio), P-MRK (1:1000 WL03553, Wanleibio), ERK (1:1000 WL01770, Wanleibio), P-ERK (1:1000 WLP1512, Wanleibio).

Cell proliferation assay

Cell viability was assessed using the Cell Counting Kit-8 (CCK-8) (K1076l; APExbio, USA). Briefly, 96-well plates were seeded with various groups of hPAECs. After allowing the cells to adhere for 6 h, the plates were placed under either normoxic or hypoxic conditions. Following different incubation periods, 10 μL of CCK-8 solution was added to each well and incubated for an additional 1.5 h. Finally, the absorbance of each well was measured at 450 nm using an enzyme-linked plate reader.

The proliferation of hPAECs was assessed using the 5-ethoxy-2′-vinyl (Edu) Cell Proliferation Assay Kit (K1076l; APExbio) following the manufacturer's protocol. This study used a six-well plate to inoculate 5×10^4 cells per well. Following 24 h of treatment under various conditions, 1 mL of Edu was added to each group and incubated at 37 °C for 1 h. The cells were fixed with 4% paraformaldehyde for 20 min, followed by incubation with 0.5 mL of the selected click reaction solution per well for 30 min. Finally, the cells were stained with DAPI for 10 min to facilitate visualization for analysis. The experiment was conducted at least three times to ensure the reliability of the results.

Cell migration assay

The cell migration experiments were conducted using Transwell and cell scratch assays. A total of 5×10^5 cells were seeded into each well of a six-well culture plate and allowed to grow until they reached confluence. Following different treatments, a clean 200 μL pipette tip was used to scrape a line across each cell layer. Subsequently, the cells were subjected to three rounds of PBS washing and cultured in a serum-free medium for 12 h. The migration width was measured using an inverted optical microscope (IX71, Olympus Corporation, Japan), and the images were captured at 0 and 12 h. Transwell assays were conducted using 24-well plates following the manufacturer's protocols. Initially, the top chamber contained 200 μL of FBS-free cell suspension, comprising 10,000 cells, and the bottom chamber was filled with 600 μL of FBS-containing medium. After various treatment conditions, the cells were fixed with 4% paraformaldehyde and subsequently stained with 1% crystal violet for 15 min. A cotton swab was employed to remove nonmigrated cells from the top surface of the membrane. Finally, the cells were quantified using a light microscope. Each experiment was performed with a minimum of four independent replicates.

Measurement of EGFR mRNA stability

Human pulmonary artery endothelial cells, subjected to different treatments, were incubated with actinomycin D for 0, 2, 4, or 6 h, followed by RNA extraction. The half-life of EGFR mRNA was analyzed using qRT-PCR, following the methodology described earlier.

Statistical analysis

The data were presented as mean ± standard deviation. Each sample was considered independent, even those measured over time within the experimental group. Statistical analysis was performed using Graph Pad Prism 9.0. The two samples were compared using the Student *t* test, assuming normal distributions.For analyses involving more than two samples, a one-way analysis of variance with Tukey's post hoc test was used. Each experiment was performed in at least three replicates. A P value < 0.05 indicated a statistically significant difference.

Results

Elevated EGLN3 levels in PAECs were correlated with the severity of PH

We analyzed the GSE163827 dataset to investigate the changes in protein expression in hPAECs following hypoxic injury so as to identify new targets for PH treatment. Our analysis revealed that EGLN3 expression was significantly upregulated after hypoxic injury (Fig. 1A). We examined lung samples from patients with PH, mice

with hypoxia-induced PH, and rats with MCT-induced PH and compared them with those in respective control groups to further validate the upregulation of EGLN3 in patients with PH and animal models. We observed elevated levels of EGLN3 mRNA in the lungs of patients with PH (Fig. 1B), mice (Fig. 1C), and rats (Fig. 1D) compared with the lungs of the controls. These findings were corroborated at the protein level (Fig. 1E–G). Given that the pathological manifestations of PH include the thickening and occlusion of distal blood vessels, we aimed to examine EGLN3 expression in distal PAECs. The immunofluorescence analysis of rat lung tissue revealed that EGLN3 co-localized with von Willebrand factor (an endothelial cell marker). The model group exhibited a higher fluorescence intensity than the control group (Fig. 1H). We conducted a detailed analysis of hypoxia- and MCT-induced lung tissue in animal models to evaluate the correlation between EGLN3 expression and disease severity. Our findings showed that EGLN3 expression increased at various time points during pulmonary artery induction in both rats and mice (Fig. 1I, J). Furthermore, Pearson correlation analysis revealed a positive correlation between EGLN3 mRNA levels in the lungs of rats and mice and RVSP levels, a critical indicator of disease severity (Fig. 1K, L).

EGLN3 knockdown inhibited the proliferation and migration of hPAECs

We assessed EGLN3 expression in hPAECs under various conditions inducing endothelial dysfunction. As shown in Fig. 2A, EGLN3 expression in hPAECs was influenced by VEGF, hypoxia, serum deprivation, and TNF-α. We performed EGLN3 knockdown and evaluated its efficiency to further investigate the role of EGLN3 (Fig. 2B). Subsequently, we assessed cell proliferation across various treatment groups via CCK8 and EdU assays. The hypoxia group demonstrated a significant increase in cell proliferation compared with the normoxia group. In contrast, the hypoxia + shEGLN3 group exhibited markedly lower cell proliferation than the hypoxia + shNC group, as indicated by the decline in the cell proliferation curve (Fig. 2C) and the reduction in the number of EdU-positive cells (Fig. 2D). No significant differences were noted among the other groups. The scratch assay was used to assess cell migration capability, revealing that the hypoxia group exhibited greater migration distance than the normoxia group after 12 h. However, the migration distance in the hypoxia + shEGLN3 group was less than that in the hypoxia + shNC group (Fig. 2E), suggesting that EGLN3 knockdown impaired cell migration ability. Similar results were observed in the Transwell assay (Fig. 2F).

EGLN3 overexpression promoted the proliferation and migration of PAECs

Following the overexpression of EGLN3 in hPAECs (Fig. 1A), we assessed their proliferation and migration capabilities. The results showed that the ovEGLN3 group exhibited significantly enhanced cell proliferation under hypoxic conditions compared with the ovNC group (Fig. S1B, S1C). Similarly, the hypoxia-ovEGLN3 group exhibited markedly improved cell migration compared with the hypoxia + ovNC group (Fig. S1D, S1E).

EGLN3 promoted hPAEC proliferation and migration through the PI3K/Akt and MAPK signaling pathways

We divided endothelial cells into two groups: hypoxia + shNC and hypoxia + shEGLN3, to further elucidate the specific mechanisms by which EGLN3 regulates proliferation and migration. We then performed transcriptome sequencing and identified 293 upregulated and 265 downregulated genes (Fig. 3A). GO and KEGG enrichment analyses of these genes revealed the inhibition of biological functions such as endothelial cell proliferation, response to oxygen levels, and cell–cell junction formation (Fig. 3B, C). Additionally, the PI3K/Akt and MAPK signaling pathways were inhibited (Fig. 3D). Further experimental validation showed that these pathways were activated in the hypoxia group compared with the normoxia group. The activation of these pathways was significantly reduced upon EGLN3 knockdown (Fig. 3E, F). Conversely, EGLN3 overexpression activated the PI3K/Akt and MAPK signaling pathways (Fig. S2A and S2B). We overexpressed EGLN3 and treated the cells with LY294002 (a PI3K/Akt inhibitor) or U0126 (a MAPK signaling pathway inhibitor) to confirm the vital role of these pathways in EGLN3-mediated promotion of

(See figure on next page.)

Fig. 1 EGLN3 elevation in PAECs correlates with PAH severity. **A** Differentially expressed proteins in the GSE163827 data set, red represents up-regulated expression, green represents down-regulated expression **B** The lungs of mice with hypoxia-induced PH EGLN3 mRNA expression. **C** The lungs of rat with MCT-induced PH EGLN3 mRNA expression. **D** EGLN3 mRNA expression in PH patients' lungs. **E** The lungs of mice with hypoxia-induced PH EGLN3 protein expression. **F** The lungs of rat with MCT-induced PH EGLN3 protein expression. **G** EGLN3 protein expression in PH patients' lungs. **H** Quantification of EGLN3 and VWF signaling localization in the pulmonary vasculature. Scale bar, 5 μm. **I** Quantification of EGLN3 levels in hypoxia-induced PH. **J** Quantification of EGLN3 levels in MCT-induced PAH. **K** and **L** The association between EGLN3 mRNA levels (normalized to β-actin) in lung tissues and RVSP during PH development is demonstrated by Pearson comparison analysis. $^{*}P < 0.05$, $^{**}P < 0.01$,. $^{***}P < 0.001$

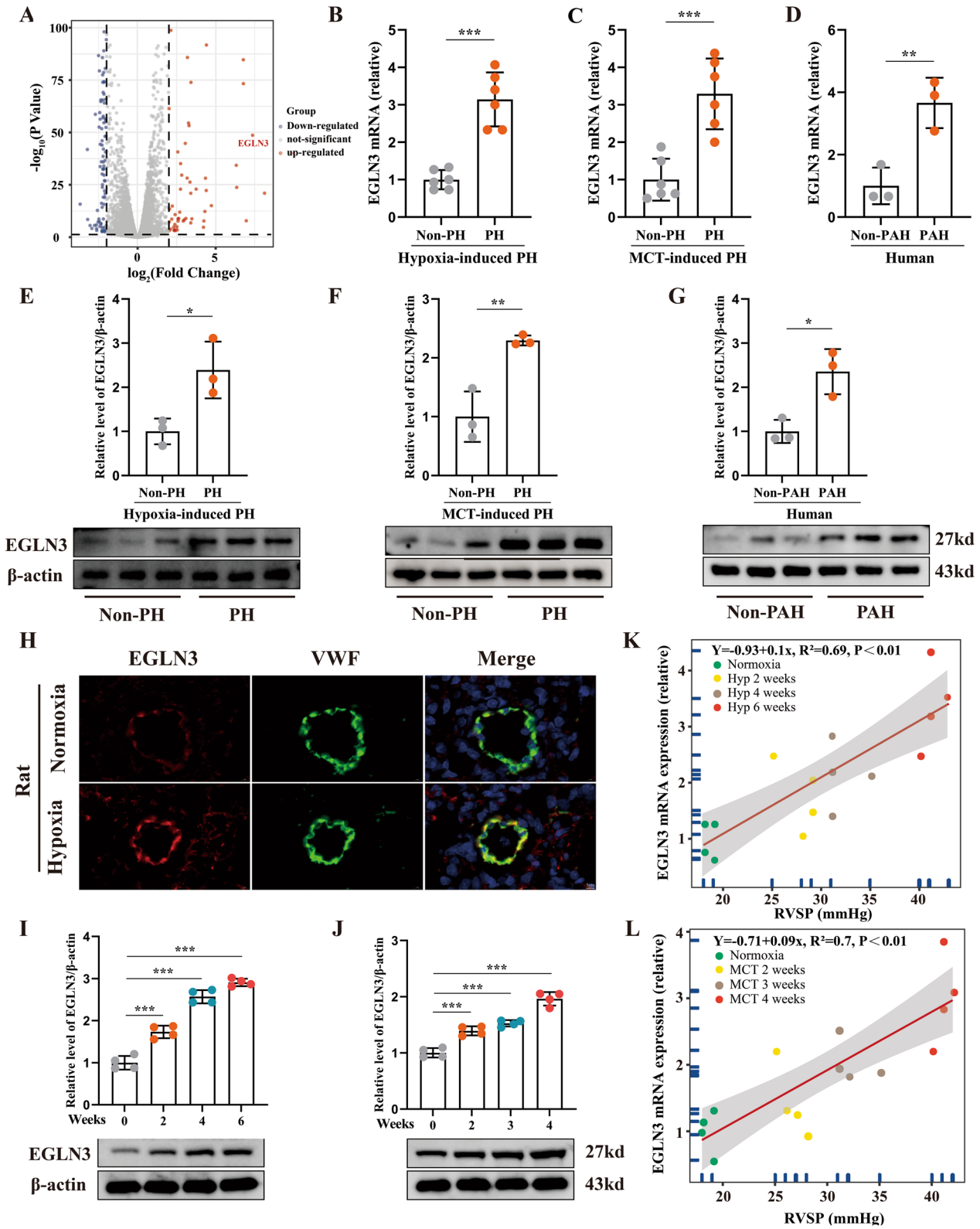

Fig. 1 (See legend on previous page.)

cell proliferation and migration. The results showed that both LY294002 and U0126 attenuated the proliferation and migration of cells induced by EGLN3 overexpression (Fig. S3A, S3B).

EGLN3 enhanced EGFR expression, promoting cell proliferation and migration

EGLN3 enhanced EGFR expression, thereby promoting cell proliferation and migration. We focused on EGFR, MET, PDGFR, and VEGFR to identify the potential targets of EGLN3 in hPAECs, as these receptors are positioned upstream of the PI3K/Akt and MAPK signaling pathways and are involved in the progression of PH [15–18]. We assessed the expression of these receptors following EGLN3 knockdown and observed significant changes in the mRNA and protein levels of EGFR (Fig. 4A, B). Based on these findings, we hypothesized that EGFR played a crucial role in EGLN3 functionality and proceeded to knock down EGFR (Fig. 4C). Our results showed that EGFR knockdown mitigated the activation of the PI3K/Akt and MAPK signaling pathways induced by EGLN3 overexpression (Fig. 4D) and reduced the associated enhancement of cell proliferation and migration (Fig. 4E, F).

HUR increased EGFR mRNA stability by binding to EGLN3

We hypothesized that the hydroxylase activity of EGLN3 mediated this effect through HIF1α or HIF2α, aiming to elucidate the specific mechanism by which EGLN3 influenced EGFR expression. We performed EGLN3 knockdown while overexpressing various vectors and found that EGLN3 knockdown did not allow for the restoration of EGFR or downstream signaling pathways by either HIF1α or HIF2α overexpression. Simultaneous overexpression of EGLN3 and the EGLN3-H196A variant (which lacks hydroxylase activity) could reverse the inhibition of EGFR and its downstream signaling pathways caused by EGLN3 knockdown. This finding suggested that the function of EGLN3 was independent of its hydroxylase activity (Fig. S4A). Previous studies reported that EGLN3 influenced EGFR expression by modulating EGFR internalization or TNF-α activity in cancer [19, 20]. We overexpressed EGLN3 while administering dynasore (a dynamin-dependent endocytosis inhibitor) or inhibiting TNF-α to further explore the aforementioned role of EGLN3. Our results showed that neither dynasore nor TNF-α inhibition affected the activation of EGFR or its downstream signaling pathways (Fig. 4B). Given that EGLN3 upregulates both EGFR mRNA and protein levels, we hypothesized that EGLN3 might regulate the stability of EGFR mRNA. We measured the half-life of EGFR mRNA following EGLN3 overexpression and found that EGLN3 significantly increased the half-life of EGFR mRNA (Fig. 4G). Considering that EGLN3 is not an RNA-binding protein and cannot directly influence mRNA stability, we examined proteins known to regulate mRNA stability, specifically HUR, MSI2, IGF2BP3, YTHDF2, and ALKBH5 [21–25]. Co-IP experiments revealed the binding of EGLN3 to the HUR protein (Fig. 4H, I). Additionally, HUR bound to EGLN3 mRNA (Fig. S5A) and directly regulated the stability of EGFR mRNA (Fig. S5B). Following HUR knockdown (Fig. S6A), we observed a reduction in the proliferation and migration of endothelial cells induced by EGLN3 overexpression (Fig. S6B and S6C) and a reduction in the activation of the PI3K/Akt and MAPK signaling pathways (Fig. S6D). Moreover, EGLN3 knockdown reduced the binding affinity of HUR to EGFR mRNA (Fig. 4J). The ability of EGLN3 to enhance EGFR mRNA stability was impaired when HUR was knocked down in the presence of EGLN3 overexpression (Fig. 4K). In summary, our findings revealed that EGLN3 increased the stability of EGFR mRNA through its interaction with HUR.

JUN regulated cell proliferation and migration by enhancing EGLN3 expression

We analyzed the upstream 2000 bp of the EGLN3 promoter region using the JASPAR and PROMO databases to further elucidate the mechanisms underlying changes in EGLN3 under hypoxic conditions. This analysis identified four candidate transcription factors: JUN, XBP-1, FOXP3, and GATA-1 (Fig. 5A). Given the significant role of JUN in the onset and progression of PH, we hypothesized that JUN induced elevated expression of EGLN3. Our findings indicated that JUN overexpression activated EGLN3, EGFR, and downstream signaling pathways, which was inhibited by EGLN3 knockdown (Fig. 5B). Furthermore, JUN overexpression promoted

(See figure on next page.)

Fig. 2 Knockdown of EGLN3 reduces PAEC proliferation and migration. **A** Shows the expression levels of EGLN3 in PAECs subjected to various treatment conditions. **B** Confirms the efficiency of EGLN3 knockdown. **C** Presents the proliferation curves of cells across different treatment conditions. **D** Demonstrates the cell proliferation capabilities under these conditions, with a greater number of red dots indicating enhanced cell proliferation ability. Bar 200 μm. **E** Displays representative images of cell migration distances at 0 and 12 h across different treatment conditions. Bar 100 μm. **F** Provides representative images depicting the number of migrating cells under various treatment conditions. Bar 50 μm. $^{*}P < 0.05$, $^{**}P < 0.01$,. $^{***}P < 0.001$

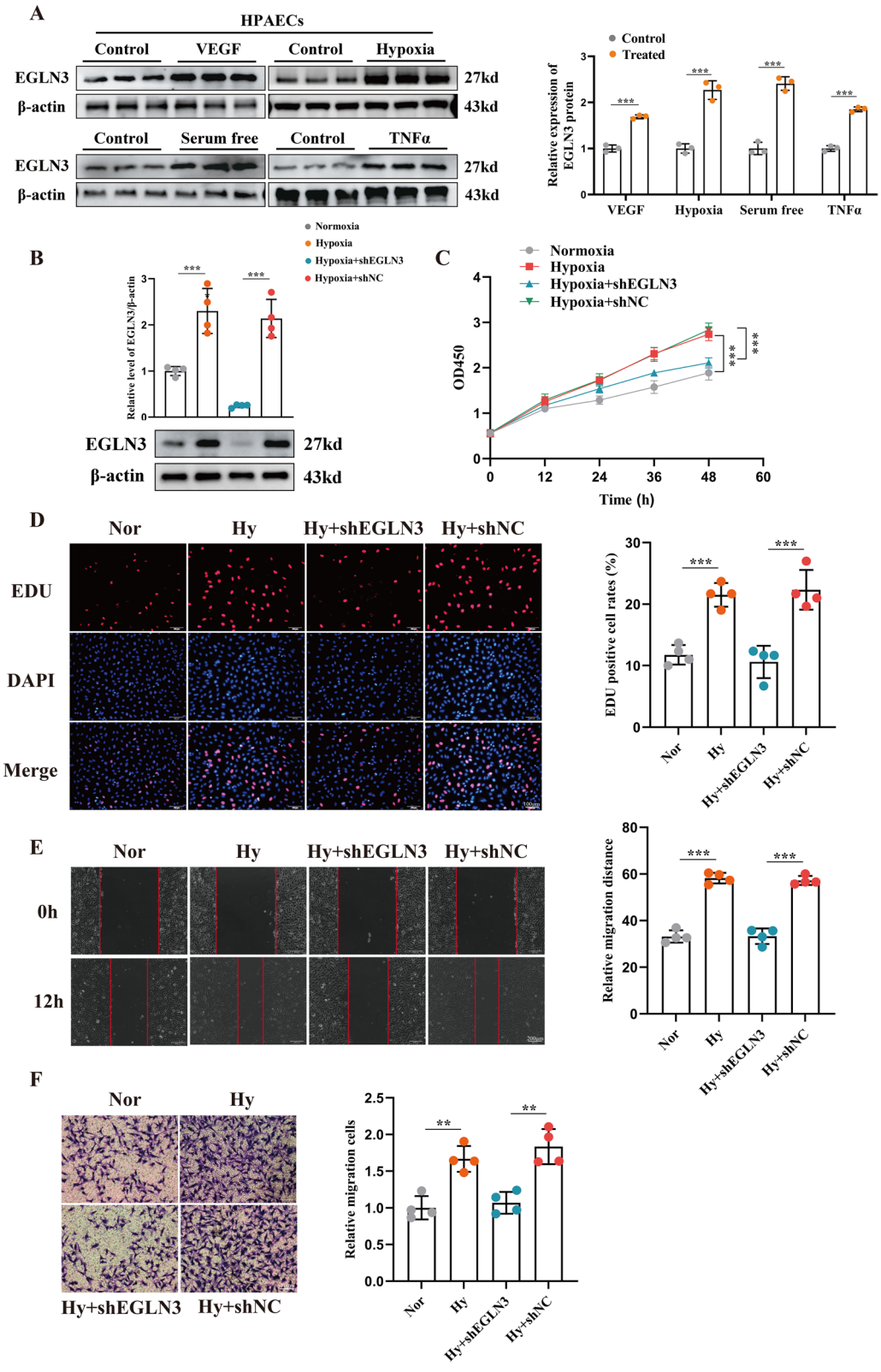

Fig. 2 (See legend on previous page.)

the proliferation and migration of endothelial cells, whereas EGLN3 knockdown mitigated this effect (Fig. S7A and S7B). We analyzed the DNA-binding motif of JUN (Fig. 5C) and the promoter region of EGLN3 (Fig. 5D). Two potential JUN-binding regions were identified. We then constructed various luciferase reporter gene vectors and co-transfected them with pcDNA3.1-JUN. The fluorescence intensity was significantly reduced for Mut1 compared with the wild type, whereas Mut2 showed no significant change relative to the wild type. Mut1,2 displayed a notable decrease in fluorescence intensity (Fig. 5E), suggesting that JUN-binding site 1 was a key site for JUN interaction with EGLN3. We performed ChIP-qPCR experiments to further confirm this hypothesis, revealing substantial amplification of fragments from JUN-binding site 1 in the EGLN3 pull-down mRNA (Fig. 5F). These results supported the conclusion that JUN enhanced EGLN3 transcription by binding to the EGLN3 promoter region between− 740 and− 755 bp.

Knocking out EGLN3 mitigated PH progression

We created endothelial-specific EGLN3 knockout mice ($EGLN3^{EC-KO}$) and developed a PH model to explore whether EGLN3 could be a viable therapeutic target for PH (Fig. 6A). Verification of the knockout efficiency revealed a significant reduction in EGFR expression in the absence of EGLN3 (Fig. 6B). Additionally, we used immunofluorescence to evaluate the proliferation of PAECs. Our findings indicated that the pulmonary blood vessels in hypoxia + $EGLN3^{WT}$ mice exhibited significantly greater endothelial cell proliferation compared with those in hypoxia + $EGLN3^{EC-KO}$ mice, with no notable differences observed in the normoxia group (Fig. 6C). Additionally, hypoxia + $EGLN3^{WT}$ mice showed substantial pulmonary vascular remodeling and inflammatory infiltration. In contrast, vascular remodeling was markedly improved in hypoxia + $EGLN3^{EC-KO}$ mice (Fig. 6D). We observed significant thickening of the right ventricular wall and an increase in cardiomyocyte width in hypoxia + $EGLN3^{WT}$ mice to further assess right ventricular remodeling. Both right ventricular wall thickness and cardiomyocyte width showed significant improvement in hypoxia + $EGLN3^{EC-KO}$ mice (Fig. 6E). Additionally, RVSP and RVHI levels were reduced following EGLN3 knockout (Fig. 6F, G). Vascular remodeling also showed some improvement, with enhanced WT% and WA% (Fig. 6H, I). Besides morphological assessments, we evaluated motor function and found that hypoxia + $EGLN3^{WT}$ mice exhibited significantly weaker motor functions than hypoxia + $EGLN3^{EC-KO}$ mice (Fig. 6J). In summary, EGLN3 knockout significantly ameliorated PH, both morphologically and functionally.

Overexpression of EGLN3 accelerated PH progression

We developed an animal model as described to determine whether EGLN3 overexpression accelerated the progression of pulmonary arterial hypertension (Fig. 7A) and confirmed the efficiency of EGLN3 overexpression via Western blot analysis. PAECs with EGLN3 overexpression showed increased EGFR levels 2 weeks after MCT induction compared with that in the control overexpression group (Fig. 7B). No significant differences were found between the normoxia groups. Additionally, endothelial cell proliferation was significantly higher in the EGLN3 overexpression group than in the control group (Fig. 7C). Examination of pulmonary blood vessel remodeling showed that EGLN3 overexpression markedly exacerbated vascular remodeling associated with PH, evidenced by increased distal vessel muscularization and luminal stenosis (Fig. 7D). Furthermore, EGLN3 overexpression led to thickening of both the right ventricular wall and myocardial fibers (Fig. 7E). We evaluated additional cardiac and vascular indicators to determine whether EGLN3 overexpression exacerbated PH. Both RVSP and RVHI significantly increased following EGLN3 overexpression (Fig. 7F, G). Similarly, the indicators of vascular remodeling, including WT% and WA%, showed substantial increases (Fig. 7H, I). Moreover, the exercise capacity of the rats was markedly reduced (Fig. 7J). In summary, our study demonstrated that EGLN3 overexpression accelerated PH progression.

Discussion

In this study, we showed the upregulation of EGLN3 in PH. JUN promoted the transcription of EGLN3 by binding to its promoter region. Additionally, EGLN3 enhanced the stability of EGFR mRNA through its interaction with HUR, leading to the activation of the

(See figure on next page.)

Fig. 3 EGLN3 regulates the PI3K/AKT and MEK/ERK signaling pathways. **A** RNA-seq technology is employed to detect differential mRNA expression between the hypoxia + shNC group and the hypoxia + shEGLN3 group. **B** Several biological processes are identified where differential proteins are predominantly enriched. **C** Differential proteins are primarily concentrated in specific cellular components. **D** Various signaling pathways are highlighted where differential proteins show significant enrichment. **E** Activation levels of the PI3K/AKT signaling pathway are compared across different groups. **F** The activation of the MEK/ERK signaling pathway is also assessed among the various groups. $^{*}P < 0.05$, $^{**}P < 0.01$, $^{***}P < 0.001$

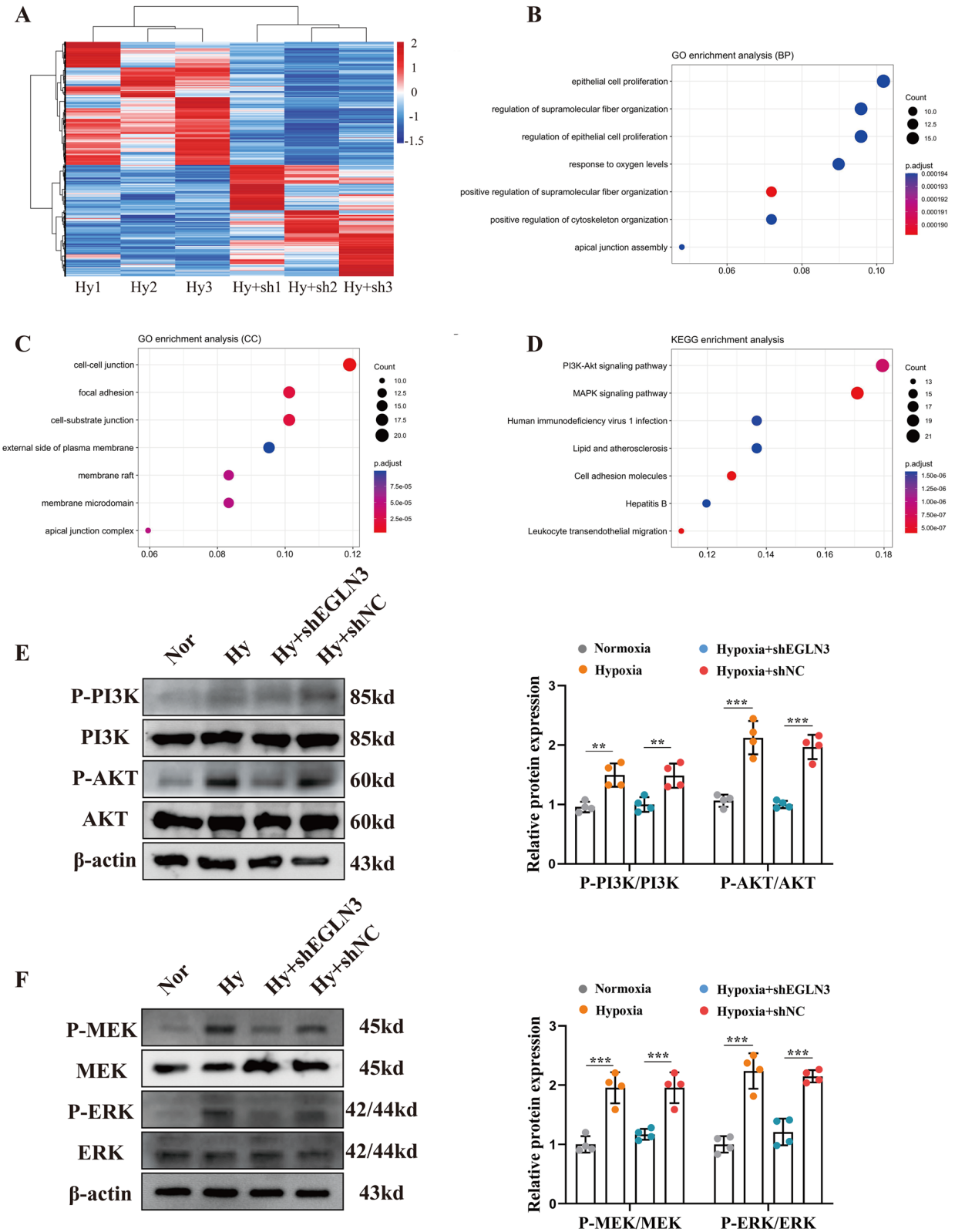

Fig. 3 (See legend on previous page.)

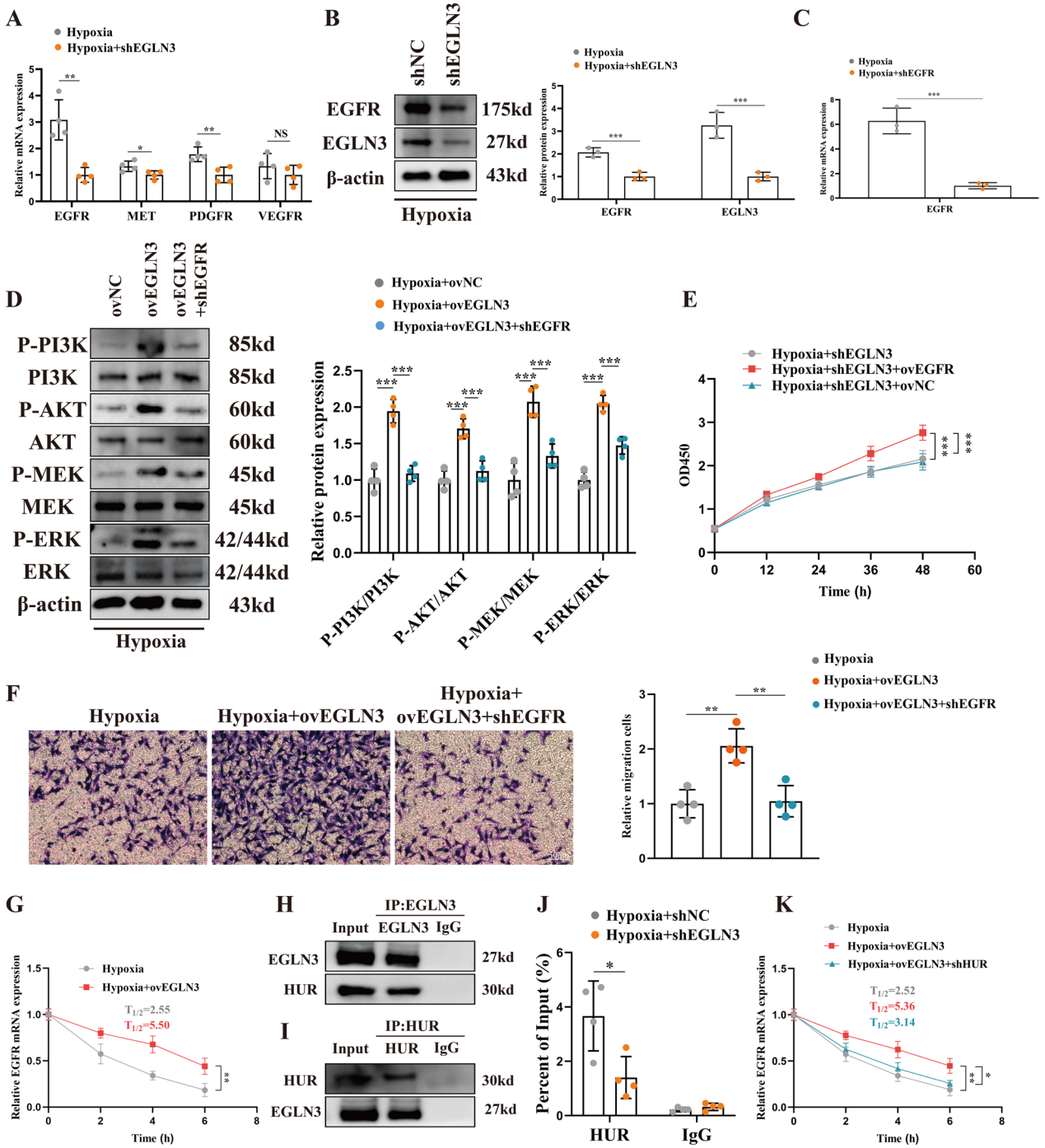

Fig. 4 EGLN3 binds HUR to positively regulate the stability of EGFR. **A** The expression levels of various receptor tyrosine kinases (RTKs) mRNA following the knockdown of EGLN3 are presented. **B** The protein expression of EGFR post-EGLN3 knockdown is shown. **C** The efficiency of EGFR knockdown is verified. **D** The activation of the PI3K/AKT and MEK/ERK signaling pathways was assessed under different treatment conditions. **E** The effects of various treatment conditions on cell proliferation were evaluated. **F** Cell migration was measured following different treatment conditions. Bar 50 μm. **G** The expression of EGFR mRNA at various time points under distinct treatment conditions reflects the changes in EGFR mRNA stability. **H** An EGLN3 antibody was utilized to pull down the protein, allowing for the detection of HUR expression. **I** The HUR antibody was used to pull down the protein to assess the expression of EGLN3. **J** Under varying treatment conditions, HUR antibodies or IgG were employed to pull down the mRNA, followed by PCR amplification to detect EGFR mRNA expression. **K** The stability of EGFR mRNA was evaluated under different treatment conditions. $^{*}P < 0.05$, $^{**}P < 0.01$,.$^{***}P < 0.001$

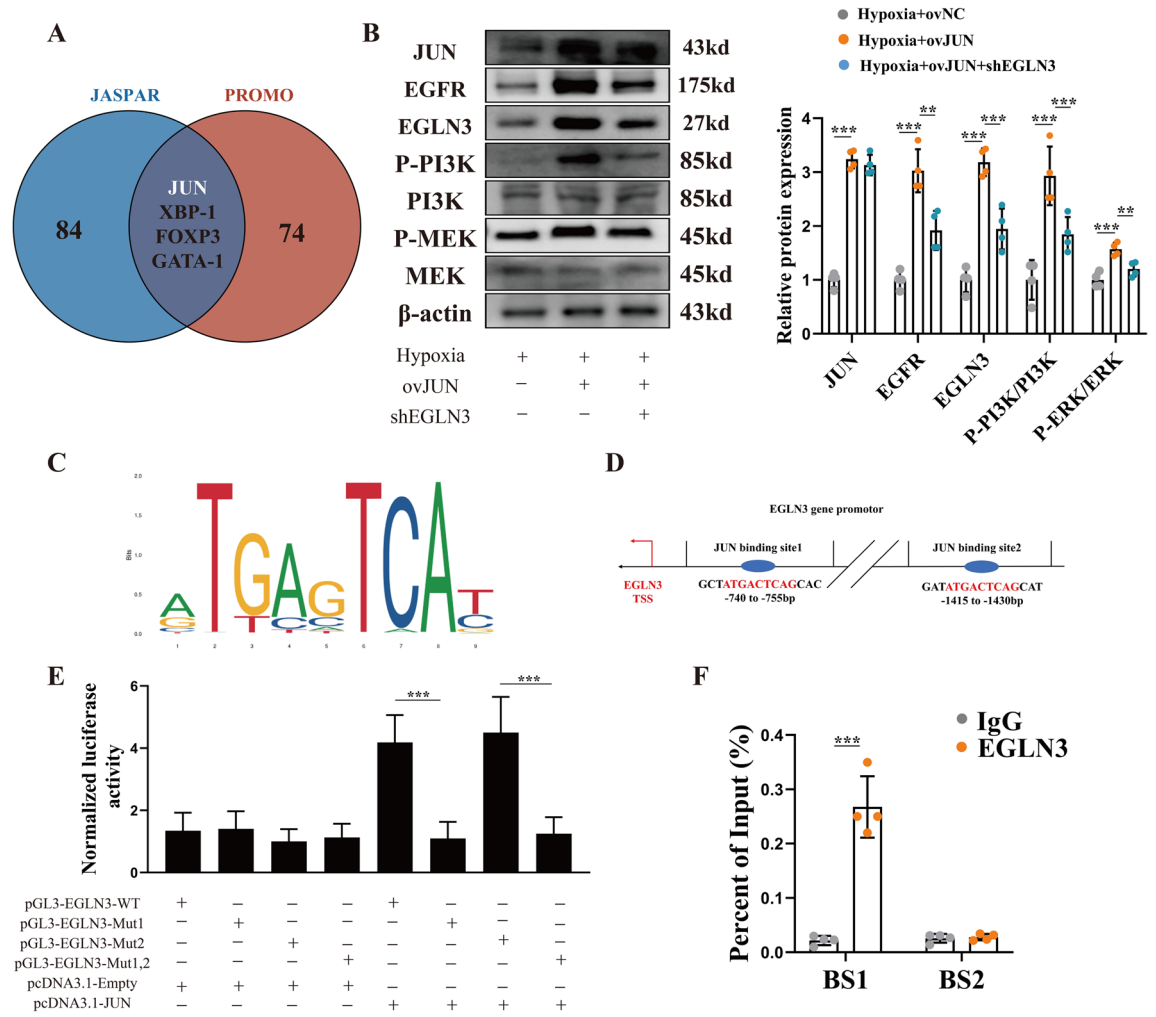

Fig. 5 JUN binds to the EGLN3 promoter region to promote EGLN3 transcription under hypoxic conditions. **A** The JASPAR and PROMO databases predict the transcription factors that can bind to the EGLN3 promoter region, and the intersection of these predictions is analyzed. **B** Following various treatment conditions, the activation of EGFR, EGLN3, and associated signaling pathways was assessed. **C** The DNA binding motif of the JUN protein is presented. **D** Sequences predicted to bind JUN within the EGLN3 promoter region are detailed. **E** Different vectors were constructed and co-transfected into endothelial cells, allowing for the detection of fluorescent protein expression in each experimental group. **F** The specific binding of EGLN3 to the promoter region was confirmed using CHIP-qPCR technology. $^{*}P<0.05$, $^{**}P<0.01$,.$^{***}P<0.001$

PI3K/Akt and MAPK signaling pathways. These pathways facilitated the proliferation and migration of PAECs (Fig. 8). Overall, our findings elucidated a critical mechanism by which PAECs contributed to PH progression through EGLN3 expression.

PH is a complex process characterized by endothelial and smooth muscle cell alterations; it involves genetic,

(See figure on next page.)

Fig. 6 Endothelium-specific knockout of EGLN3 alleviates the progression of PH. **A** The timeline for establishing the mouse model of PH is presented. **B** Verification of EGLN3 and EGFR protein expression levels in various mouse groups is shown. **C** Multiple staining of VWF and PCNA was conducted to assess the proliferation capability of PAECs across the different groups. Bar 20 μm. **D** HE staining, along with immunofluorescence staining, was employed to evaluate vascular remodeling among the groups. Bar 50 μm. **E** HE staining was used to assess right ventricular wall thickening across the different groups. Bar 1 mm. **F** and **G** Differences in RVSP and RVHI among the groups were measured. **H** and **J** Differences in the percentage of WT% and WA% among the groups were analyzed. **J** The distance traveled by mice in various groups on the treadmill was recorded to reflect their cardiac function. $^{*}P<0.05$, $^{**}P<0.01$,.$^{***}P<0.001$

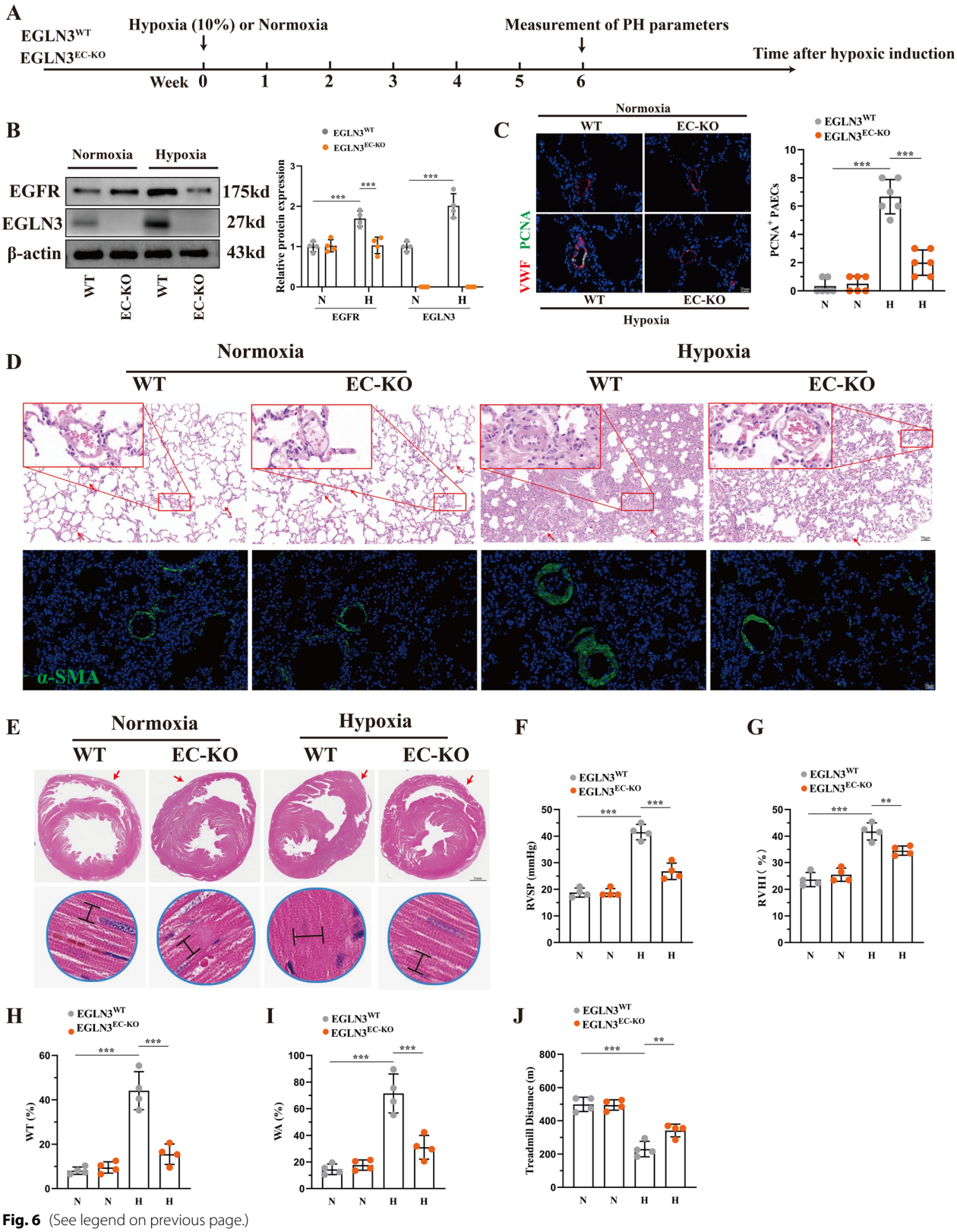

Fig. 6 (See legend on previous page.)

epigenetic, and microenvironmental changes driving markers for proliferation and migration [26]. Endothelial dysfunction has emerged as a crucial factor in PH-associated vascular remodeling. PAECs not only act as a natural barrier within blood vessels but also release various mediators that regulate vasoconstriction and smooth muscle cell growth, influencing smooth muscle cell function [5]. This study aimed to identify a novel target within PAECs for potential intervention in PH.

Hypoxia is widely recognized as a primary causative factor of PH, with EGLN3 serving as a key hypoxia sensor. EGLN3 is crucial in various conditions, including cancer and diabetes [8]. EGLN3 modulates EGFR expression by affecting EGFR endocytosis or TNF-α activity, which influences the proliferation and migration of cancer cells. Additionally, EGLN3 is well known for its hydroxylase activity; it regulates hypoxic responses through the hydroxylation of HIF1α and HIF2α [27]. This demonstrated that EGLN3-mediated proliferation and migration in PAECs occurred independently of its hydroxylase activity and did not involve the modulation of EGFR endocytosis or TNF-α activity. We proposed a novel regulatory mechanism in which EGLN3 stabilized EGFR mRNA through its interaction with HUR, a finding that was not previously reported. This differential regulation of molecules across various cell types allowed EGLN3 to perform distinct functions in various tissues. We conducted endothelial cell–specific knockdown experiments to explore EGLN3 as a potential therapeutic target for PH, revealing a significant improvement in PH progression. Our findings support the potential of EGLN3 as a therapeutic target. Although EGLN3-specific targeted inhibitors are currently under development, pharmacological knockdown studies with these agents have not been conducted yet. Future research will address this limitation.

HUR regulates EGFR expression post-transcriptionally [21, 28]. However, the precise mechanism through which HUR mediates mRNA stability remains poorly understood. HUR is mainly located in the nucleus of unstimulated cells but can translocate to the cytoplasm upon cellular stimulation, which is a process associated with the stability of various target mRNAs [29]. This study found that HUR bound to EGFR mRNA and participated in its stability regulation, which was consistent with previous findings. Additionally, we discovered that EGLN3 bound to HUR, which enhanced its interaction with EGFR mRNA. This interaction stabilized EGFR mRNA and contributed to cell proliferation and migration.

We predicted and experimentally confirmed that JUN was a key regulator of EGLN3 expression, aiming to understand the changes in EGLN3 expression under hypoxic conditions. JUN is crucial in the onset and progression of PH, influencing cell proliferation and growth of blood vessels [30]. Our findings showed that JUN activated the MAPK signaling pathway by impacting EGLN3 expression. The MAPK signaling pathway also regulated the phosphorylation and transcriptional activation of JUN itself. Therefore, this study suggested that this signaling pathway axis might establish a positive feedback loop, promoting the proliferation and migration of PAECs.

The limitations of this study are as follows: ① Obtaining clinical samples from patients with pulmonary arterial hypertension is particularly challenging. The clinical samples collected in this study are limited in size and require further validation with larger clinical cohorts to enhance the rigor of the findings. ② Currently, there is no effective EGLN3-specific inhibitor available, which has hindered our ability to conduct pharmacological experiments. We believe that the therapeutic effects of EGLN3-targeted inhibition should be demonstrated both prior to and following the onset of pulmonary arterial hypertension. ③ Additionally, this article has not yet explored the binding site for mechanism-level research. We hope to address these limitations in future investigations.

Conclusions

This study identified EGLN3 as a promising new target for treating PH and investigated its role in the pathogenesis of the disease. JUN enhanced EGLN3 transcription under hypoxic conditions, leading to increased binding of EGLN3 to HUR. This interaction stabilized EGFR mRNA, activated downstream signaling pathways, and promoted the proliferation and migration of

(See figure on next page.)

Fig. 7 Overexpression of EGLN3 aggravates the progression of PH **A** The timeline for establishing the rat model of PH is presented. **B** Verification of EGLN3 and EGFR protein expression levels in various rat groups is shown. **C** Multiple staining of VWF and PCNA was conducted to assess the proliferation capability of PAECs across the different groups. Bar 20 μm. **D** HE staining, along with immunofluorescence staining, was employed to evaluate vascular remodeling among the groups. Bar 50 μm. **E** HE staining was used to assess right ventricular wall thickening across the different groups. Bar 1 mm. **F** and **G** Differences in RVSP and RVHI among the groups were measured. **H** and **J** Differences in the percentage of WT% and WA% among the groups were analyzed. **J** The distance traveled by rats in various groups on the treadmill was recorded to reflect their cardiac function. $^{*}P < 0.05$, $^{**}P < 0.01$, $^{***}P < 0.001$

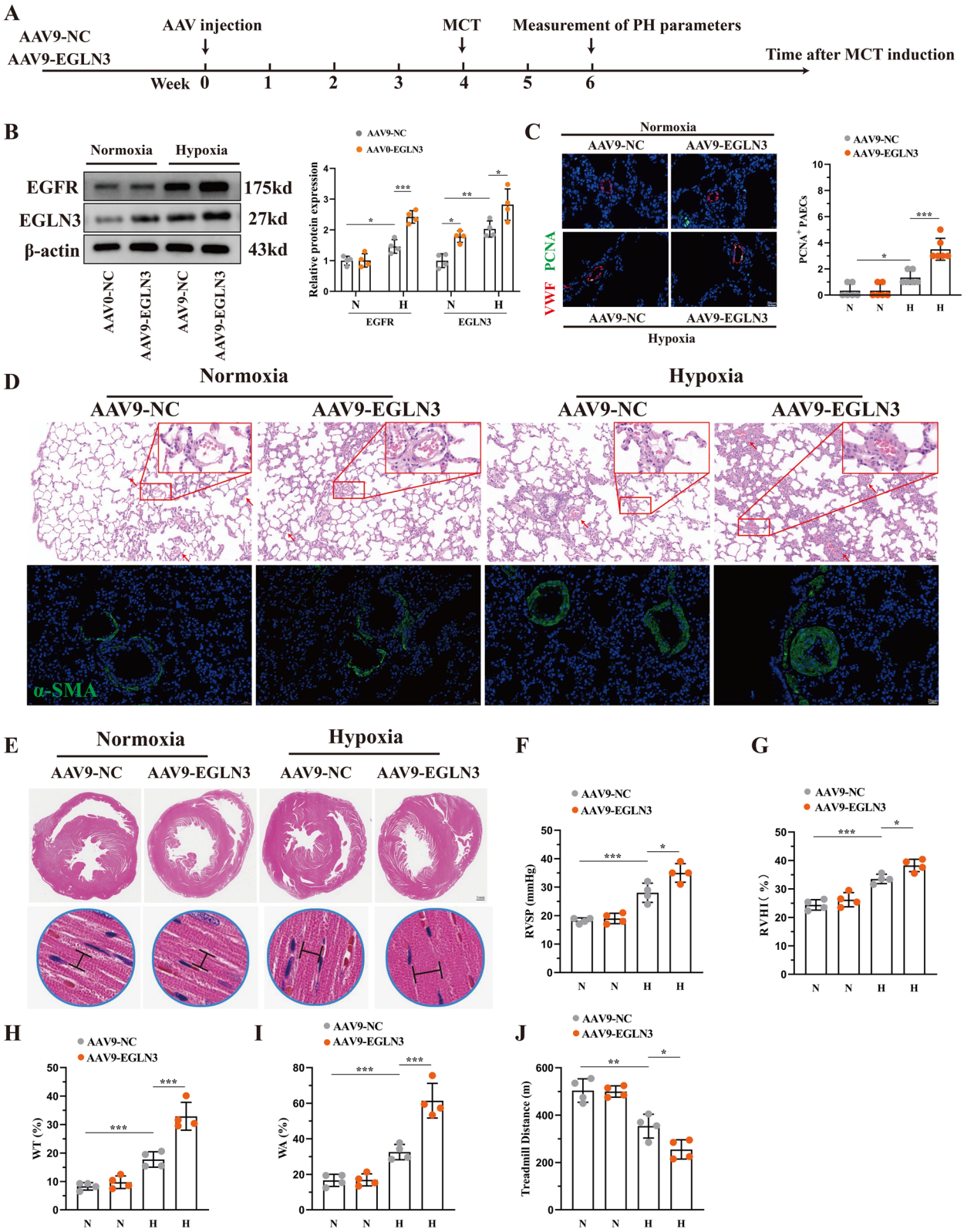

Fig. 7 (See legend on previous page.)

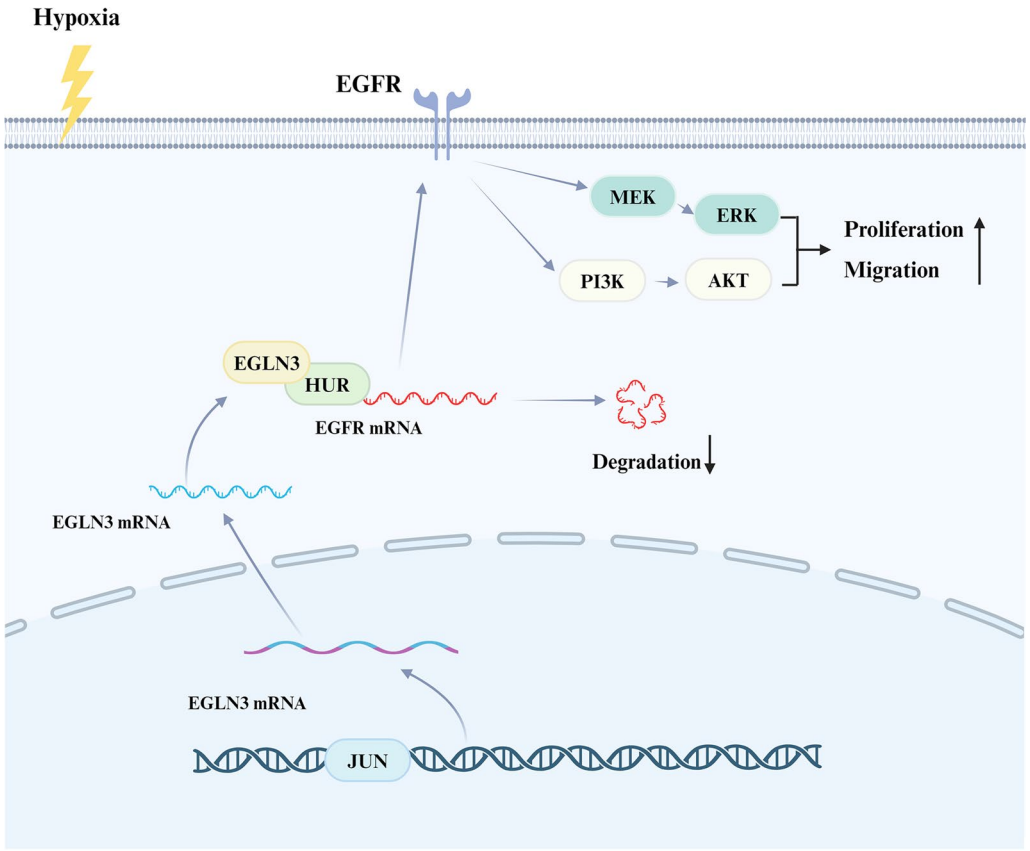

Fig. 8 Graphical Abstract Under hypoxic conditions, JUN enhances the transcription of EGLN3, which subsequently binds to HUR to positively regulate the stability of EGFR mRNA. This interaction activates the PI3K/AKT and MEK/ERK signaling pathways, ultimately promoting the proliferation and migration of endothelial cells

PAECs. These findings provide novel insights into the development of PH and establish a theoretical foundation for its treatment.

Supplementary Information

The online version contains supplementary material available at https://doi.org/10.1186/s12931-025-03144-6.

Supplementary material 1.

Author contributions

Yi Liu designed the study, conducted the experiments, interpreted the results, and wrote the manuscript. Qing Que and Bo Li and Qiang Hu conducted the experiments and interpreted the results. Kunchi Zhang, Nianlong Yang conducted the experiments. Xiaodong Deng, Sheng Lv designed the study and revised the manuscript. All authors read and approved the final manuscript.

Funding

This study received support from the Sichuan Scientific Research Project Program (grant no. S2024029) alongside the Panzhihua Science and Technology Program (grant no. 2023ZD-S-11).

Availability of data and materials

No datasets were generated or analysed during the current study.

Declarations

Ethics approval and consent to participate

The ethics committee of the First Affiliated Hospital at Jinzhou Medical University approved the study protocol regarding tissue donation; also, written informed consent was obtained from either the patients involved or their appointed next of kin (2024216). Additionally, the Research Ethics Committee at Jinzhou Medical University granted approval for all animal experiments and methodologies (2021083001). The Laboratory Animal Science Department facilitated the procurement of Sprague–Dawley rats. Strict compliance with the established protocols for the care and use of laboratory animals was maintained throughout all experimental processes.

Consent for publication

All authors consent to the publication of this manuscript.

Competing interests

The authors declare no competing interests.

Author details

[1]Department of Critical Care Medicine, Panzhihua Central Hospital, Panzhihua 61700, China.

Received: 5 October 2024 Accepted: 9 February 2025
Published online: 21 February 2025

References

1. Mocumbi A, Humbert M, Saxena A, Jing ZC, Sliwa K, Thienemann F, Archer SL, Stewart S. Pulmonary hypertension. Nat Rev Dis Primers. 2024;10:1.
2. Olsson KM, Corte TJ, Kamp JC, Montani D, Nathan SD, Neubert L, Price LC, Kiely DG. Pulmonary hypertension associated with lung disease: new insights into pathomechanisms, diagnosis, and management. Lancet Respir Med. 2023;11:820–35.
3. Cullivan S, Gaine S, Sitbon O. New trends in pulmonary hypertension. Eur Respir Rev. 2023;32:10.
4. Naeije R, Richter MJ, Rubin LJ. The physiological basis of pulmonary arterial hypertension. Eur Respir J. 2022;59:10.
5. Evans CE, Cober ND, Dai Z, Stewart DJ, Zhao YY. Endothelial cells in the pathogenesis of pulmonary arterial hypertension. Eur Respir J. 2021;58:10.
6. Pokharel MD, Marciano DP, Fu P, Franco MC, Unwalla H, Tieu K, Fineman JR, Wang T, Black SM. Metabolic reprogramming, oxidative stress, and pulmonary hypertension. Redox Biol. 2023;64: 102797.
7. Strocchi S, Reggiani F, Gobbi G, Ciarrocchi A, Sancisi V. The multifaceted role of EGLN family prolyl hydroxylases in cancer: going beyond HIF regulation. Oncogene. 2022;41:3665–79.
8. Cai F, Yang X, Ma G, Wang P, Zhang M, Zhang N, Zhang R, Liang H, Nie Y, Dong C, Deng J. EGLN3 attenuates gastric cancer cell malignant characteristics by inhibiting JMJD8/NF-kappaB signalling activation independent of hydroxylase activity. Br J Cancer. 2024;130:597–612.
9. Chen W, Song J, Liu S, Tang B, Shen L, Zhu J, Fang S, Wu F, Zheng L, Qiu R, et al. USP9X promotes apoptosis in cholangiocarcinoma by modulation expression of KIF1Bbeta via deubiquitinating EGLN3. J Biomed Sci. 2021;28:44.
10. Montani D, Chaumais MC, Guignabert C, Gunther S, Girerd B, Jais X, Algalarrondo V, Price LC, Savale L, Sitbon O, et al. Targeted therapies in pulmonary arterial hypertension. Pharmacol Ther. 2014;141:172–91.
11. Berghausen EM, Janssen W, Vantler M, Gnatzy-Feik LL, Krause M, Behringer A, Joseph C, Zierden M, Freyhaus HT, Klinke A, et al. Disrupted PI3K subunit p110alpha signaling protects against pulmonary hypertension and reverses established disease in rodents. J Clin Invest. 2021. https://doi.org/10.1172/JCI136939.
12. Xiong Y, Wang Y, Yang T, Luo Y, Xu S, Li L. Receptor tyrosine kinase: still an interesting target to inhibit the proliferation of vascular smooth muscle cells. Am J Cardiovasc Drugs. 2023;23:497–518.
13. Yu X, Zhao X, Zhang J, Li Y, Sheng P, Ma C, Zhang L, Hao X, Zheng X, Xing Y, et al. Dacomitinib, a new pan-EGFR inhibitor, is effective in attenuating pulmonary vascular remodeling and pulmonary hypertension. Eur J Pharmacol. 2019;850:97–108.
14. Hardie WD, Davidson C, Ikegami M, Leikauf GD, Le Cras TD, Prestridge A, Whitsett JA, Korfhagen TR. EGF receptor tyrosine kinase inhibitors diminish transforming growth factor-alpha-induced pulmonary fibrosis. Am J Physiol Lung Cell Mol Physiol. 2008;294:L1217-1225.
15. Shi Y, Hu X, Zhang S, Lv D, Wu L, Yu Q, Zhang Y, Liu L, Wang X, Cheng Y, et al. Efficacy, safety, and genetic analysis of furmonertinib (AST2818) in patients with EGFR T790M mutated non-small-cell lung cancer: a phase 2b, multicentre, single-arm, open-label study. Lancet Respir Med. 2021;9:829–39.
16. Park CS, Kim SH, Yang HY, Kim JH, Schermuly RT, Cho YS, Kang H, Park JH, Lee E, Park H, et al. Sox17 Deficiency promotes pulmonary arterial hypertension via HGF/c-met signaling. Circ Res. 2022;131:792–806.
17. Galkin A, Sitapara R, Clemons B, Garcia E, Kennedy M, Guimond D, Carter LL, Douthitt A, Osterhout R, Gandjeva A, et al. Inhaled seralutinib exhibits potent efficacy in models of pulmonary arterial hypertension. Eur Respir J. 2022. https://doi.org/10.1183/13993003.02356-2021.
18. Zhou W, Liu K, Zeng L, He J, Gao X, Gu X, Chen X, Jing Li J, Wang M, Wu D, et al. Targeting VEGF-A/VEGFR2 Y949 Signaling-Mediated Vascular Permeability Alleviates Hypoxic Pulmonary Hypertension. Circulation. 2022;146:1855–81.
19. Garvalov BK, Foss F, Henze AT, Bethani I, Graf-Hochst S, Singh D, Filatova A, Dopeso H, Seidel S, Damm M, et al. PHD3 regulates EGFR internalization and signalling in tumours. Nat Commun. 2014;5:5577.
20. Dopeso H, Jiao HK, Cuesta AM, Henze AT, Jurida L, Kracht M, Acker-Palmer A, Garvalov BK, Acker T. PHD3 controls lung cancer metastasis and resistance to EGFR inhibitors through TGFalpha. Cancer Res. 2018;78:1805–19.
21. Wang A, Bao Y, Wu Z, Zhao T, Wang D, Shi J, Liu B, Sun S, Yang F, Wang L, Qu L. Long noncoding RNA EGFR-AS1 promotes cell growth and metastasis via affecting HuR mediated mRNA stability of EGFR in renal cancer. Cell Death Dis. 2019;10:154.
22. Makhov P, Bychkov I, Faezov B, Deneka A, Kudinov A, Nicolas E, Brebion R, Avril E, Cai KQ, Kharin LV, et al. Musashi-2 (MSI2) regulates epidermal growth factor receptor (EGFR) expression and response to EGFR inhibitors in EGFR-mutated non-small cell lung cancer (NSCLC). Oncogenesis. 2021;10:29.
23. Chen LJ, Liu HY, Xiao ZY, Qiu T, Zhang D, Zhang LJ, Han FY, Chen GJ, Xu XM, Zhu JH, et al. IGF2BP3 promotes the progression of colorectal cancer and mediates cetuximab resistance by stabilizing EGFR mRNA in an m(6)A-dependent manner. Cell Death Dis. 2023;14:581.
24. Zhong L, Liao D, Zhang M, Zeng C, Li X, Zhang R, Ma H, Kang T. YTHDF2 suppresses cell proliferation and growth via destabilizing the EGFR mRNA in hepatocellular carcinoma. Cancer Lett. 2019;442:252–61.
25. Zhu H, Gan X, Jiang X, Diao S, Wu H, Hu J. ALKBH5 inhibited autophagy of epithelial ovarian cancer through miR-7 and BCL-2. J Exp Clin Cancer Res. 2019;38:163.
26. Johnson S, Sommer N, Cox-Flaherty K, Weissmann N, Ventetuolo CE, Maron BA. Pulmonary hypertension: a contemporary review. Am J Respir Crit Care Med. 2023;208:528–48.
27. Luo W, Hu H, Chang R, Zhong J, Knabel M, O'Meally R, Cole RN, Pandey A, Semenza GL. Pyruvate kinase M2 is a PHD3-stimulated coactivator for hypoxia-inducible factor 1. Cell. 2011;145:732–44.
28. Figueroa A, Cuadrado A, Fan J, Atasoy U, Muscat GE, Munoz-Canoves P, Gorospe M, Munoz A. Role of HuR in skeletal myogenesis through coordinate regulation of muscle differentiation genes. Mol Cell Biol. 2003;23:4991–5004.
29. Wu X, Xu L. The RNA-binding protein HuR in human cancer: a friend or foe? Adv Drug Deliv Rev. 2022;184: 114179.
30. Liu J, Wang W, Wang L, Chen S, Tian B, Huang K, Corrigan CJ, Ying S, Wang W, Wang C. IL-33 initiates vascular remodelling in hypoxic pulmonary hypertension by up-regulating HIF-1alpha and VEGF expression in vascular endothelial cells. EBioMedicine. 2018;33:196–210.

Publisher's Note